PROCEEDINGS, 41st Workshop on Geothermal Reservoir Engineering
Stanford University, Stanford, California, February 22-24, 2016
SGP-TR-209

High Temperature Aquifer Storage

Martina Ueckert, Reinhard Niessner and Thomas Baumann

Institute of Hydrochemistry, TUM, Marchioninistrasse 17, 81377 Munich, Germany

martina.ueckert@tum.de

Keywords: Aquifer Thermal Storage, High Temperature Storage, Carbonatic Rock, Malm Aquifer, Molasse Basin Bavaria

ABSTRACT

The storage and recuperation of hot water with injection temperatures of up to 110 °C and flow rates of 15 L/s into a carbonatic aquifer over a total time of about 530 hours is described. On-site parameters as well as cation composition were recorded continuously. By evaluating hydrochemical data not only heat recovery, but also hydrochemical reactions during withdrawal and hydraulic properties can be investigated. One of the main questions is how to control the limestone equilibrium during both, the heating process as well as the injection of the heated water back into the cold reservoir. While the first issue can be easily solved by calculating an appropriate amount of CO_2 to avoid precipitations using *PhreeqC*, the second process is harder to simulate. Not only supersaturation of the water with respect to calcium and magnesium mineral phases but also its kinetics, properties of the rock matrix as well as degassing processes role the chemical reactions in the aquifer and can therefore not be predicted by laboratory experiments alone. Evaluating the hydrochemical data allows also interpretation of hydraulic properties of the aquifer.

1. INTRODUCTION

Combined heat and power plants (CHP) are efficient and environmentally friendly because excess heat produced during power generation is used for heating purposes. While the power demand remains approximately constant throughout the year, the heat demand shows seasonal variations. In a worst-case scenario, the heat production in winter is not sufficient, and the power production in summer has to be ramped down because the excess heat cannot be released to the environment. Therefore, storage of excess heat of CHP is highly beneficial from an economic and an ecological point of view. Aquifer thermal energy storage (ATES) has been a promising technology for energy storage (Drijver et al. (2012)) for several years. Water from an aquifer is produced, heated up by excess heat and injected through a second borehole into the reservoir. Besides high water volumes, one benefits from the lower heat capacity and heat conductivity of the rock matrix which then serves as an insulator. However, while there have been several studies performed in clastic aquifers and for temperatures below 100 °C, knowledge about high injection temperatures is still limited (e.g. Hebig et al. (2012)). Thermal losses are one of the limiting processes (e.g. Yang et al. (2010)) as well as precipitations (e.g. Griffioen and Appelo (1999)). Potential problems of ATES in carbonaceous aquifers are mainly caused by the disruption of the carbonate equilibrium resulting in precipitation and dissolving processes, which are limiting the economical benefit. Establishing a conceptual model with *PhreeqC* helps to understand these processes in the aquifer but does not yet provide a full understanding of ATES.
At a car manufacturing plant a new energy supply consisting of seven CHP providing E_{El} = 31 MW and E_{Th} = 27 MW is going to be installed in 2018. In order to reduce the carbon dioxide footprint and increase the efficiency, the CHP will be connected to an ATES. Given the produced thermal energy, it is evident that only an ATES with high specific yield offers enough storage capacity. Preliminary research and geophysical soundings indicated that the Malm aquifer most likely offers these conditions. Within a research project funded by the Bavarian State Ministry for Economic Affairs the BMW Group launched a detailed site investigation including a research drill and a large scale heat storage test. The project combines field analysis with modeling and is supported by laboratory experiments. Its main objective is to guarantee a reliable transfer to other sites and to help render thermal aquifer storage more beneficial.

2. MATERIALS AND METHODS

2.1 Site Description

The underlying bed of the Molasse Basin in Bavaria is built by carbonates from the upper Jurassic (’Malm’) which are dipping towards the Alps in the south (e.g. Schmidt et al. (2005)). Favorable hydrogeological conditions like high permeabilities and flow conditions are depending on the facies and are already utilized in the southern parts of the Molasse Basin for hydro-geothermal energy production (e.g. Böhm et al. (2010)). In the eastern part of the Molasse Basin, the region Niederbayern, favorable Malm carbonates are found and therefore a research drilling was constructed at a test site NE of the city Landshut in 2014. The top of the Malm carbonates was found in 245 m b.s.l and the final depth was reached in 472.9 m b.s.l. The aquifer is sealed off by impermeable, overlying bedding which is about 140 m thick and mainly consists of claystones and sandstones. The top of the Malm aquifer is built by limestone, while the rest of the aquifer consists of dolomites and dolomitic breccia. The aquifer is flowing freely with up to 19.4 L/s, which caused drilling problems and core losses from a depth of 297 m b.s.l. to 397 m b.s.l. The cored drilling states proper data of lithology at the test site. The cation composition of the reservoir water is given in table 1.

2.2 Heat Storage Test

The heat storage test was performed in a single well borehole and was planned as push-pull-tracer test since this is a well established method for aquifer characterization in a single well borehole (e.g. Hebig et al. (2014)). Five stages of hot water injections were done in two tests, with a flow rate of 15 L/s for each injection and production stage. The 108 hours lasting pre-test was brought forward (stage 0) in a depth from 245 m b.s.l. to 297 m b.s.l. Thereby, 65 °C hot water was injected for 48 hours. After 34 hours a fluorescent dye was added (sodium fluorescein (URA)) with a concentration of 37.3 µg/L over an injection time of 3 h 40 min. After reaching the final depth, and performing a pumping test, the main test (stages 1-4) was performed over 420 hours in total. The main test consists of 4 injection pulses (60-48-48-48 hours) with 80-90-110-110 °C hot tap water and a calculated amount of CO_2 was injected (AirLiquide) before reaching the heat exchanger. Additionally three fluorescent dye pulses were added (stage 1, 3 and 4) for 3 hours (stage 1 and 3) resp. 2 hours (stage 4) via dosing pump. The fluorescent dye tracer included for each injection pulse a conservative (URA and sodium naphtionate (NAP)) and a reactive tracer (amidorhodamine G (ARG) and sulphorhodamine B (SRB)) (e.g. Kasnavia et al. (1999)). Production was performed without underground pump, while it has to be regulated to a flow rate of 15 L/s on surface. Production times were set to 48-36-36-96 hours. Produced water passed a degassing station, several cooling tanks as well as regulation stations, where pH value and oxygen content could be regulated. The plant construction was planned by Gammel Engineering, Abensberg, Germany and realized by Lausser, Rattiszell, Germany. The cation composition of the injected tap water is given in table 1.

Table 1: Major ion concentration of tap (includes variation of the cation concentration for each stage) and reservoir water

mg/L	*Tap Water (15.10.-11.12.2014)*	*Reservoir Water (6.10.2014)*
Na^+	4±0.5	157
K^+	1±0.2	14
Ca^{2+}	80±1	43
Mg^{2+}	31±1	27
Cl^-	14	136
NO_3^-	16	0.4
SO_4^{2-}	13	16
HCO_3^-	349	485

2.3 Sampling and Analysis

A bypass was installed at the test field where samples were taken and on site parameters (pH, temperature and electrical conductivity (EC)) were recorded continuously. A cooling system installed at the bypass allowed sampling at temperatures above 100 °C. In a lab container, cation concentrations were determined by Ion chromatography (C4-150 column, Metrohm, Germany) and intensities of the produced fluorecent dyes were measured in sampling intervals of down to 15 minutes with Shimadzu Spectrometer (RF-540). Acid capacity was determined by titration, redox-potential and oxygen content were measured by electrodes (Seven Go Duo resp. Seven Go Pro, Mettler Toledo). Pressure heads, temperatures, pH and EC were recorded at the well head. Additional samples were taken at the bypass to determine anion concentration, trace elements, gas composition and isotopic composition. Standards for the cation chromatography were run once per day and new standards were prepared weekly. Standard deviation of the cation calibration was for all cations less than 3 %. For the analysis in the laboratory in Munich, the percent error was given with < 1%. Measuring probes in the field laboratory were calibrated at least once per day and those installed in the bypass were calibrated during modification from injection to production stage. Calibrations of all fluorescent dyes were made with tap water from the test site. The injection of the dyes was done by technicians of the plant construction to avoid contamination of the analysists.

2.4 Hydrogeochemical Modeling

The hydrogeochemical model was implemented in *PhreeqC*, version 3.3.2, using the provided *phreeqc.dat* database. To simulate the conditioning of the tap water, CO_2 was added as REACTION until the saturation indices (SI) for each injection temperature were within 0.1-0.2 to prevent scaling in the heat exchanger. Additionally, pH-value and SI for aragonite and dolomite were added to the output file.

3. RESULTS

3.1 Conditioning of the Injected Tap Water

Before injecting the tap water of the drilling site a forward calculation of *PhreeqC* was preformed to calculate the amount of CO_2 to prevent precipitations. Therefore a $SI_{Calcite}$ between 0.1-0.2 was targeted, while the slight oversaturation was planned to avoid corrosion of pipe material. That resulted in CO_2 concentrations of 90 mg/L for injection temperature (T_{Inj}) of 65°C up to 420 mg/L for T_{Inj} of 110 °C and a resulting pH value of 6.78 resp. 6.22. The measured pH values during injection were slightly higher than the calculated ones. After a total injection volume of 13600 m³ water, neither pipes nor heat exchanger showed any precipitations or corrosions.

3.2 Hydrochemical Monitoring of the Heat Storage Test

3.2.1 Development of On-Site-Parameters

The temperature development (measured at the well head) is shown in Fig. 1. The curves start with a sharp decrease of the temperatures as soon as the water from the upper borehole has been produced. Then the temperature decreases slowly. While the temperature level reflects the injection temperatures, the higher temperature level in stage 4 shows a higher level compared to stage 3 which had the same injection temperature and indicates a significant heating of the aquifer matrix. It is visible that temperatures of the produced water increased over time, which shows the heating of the aquifer.

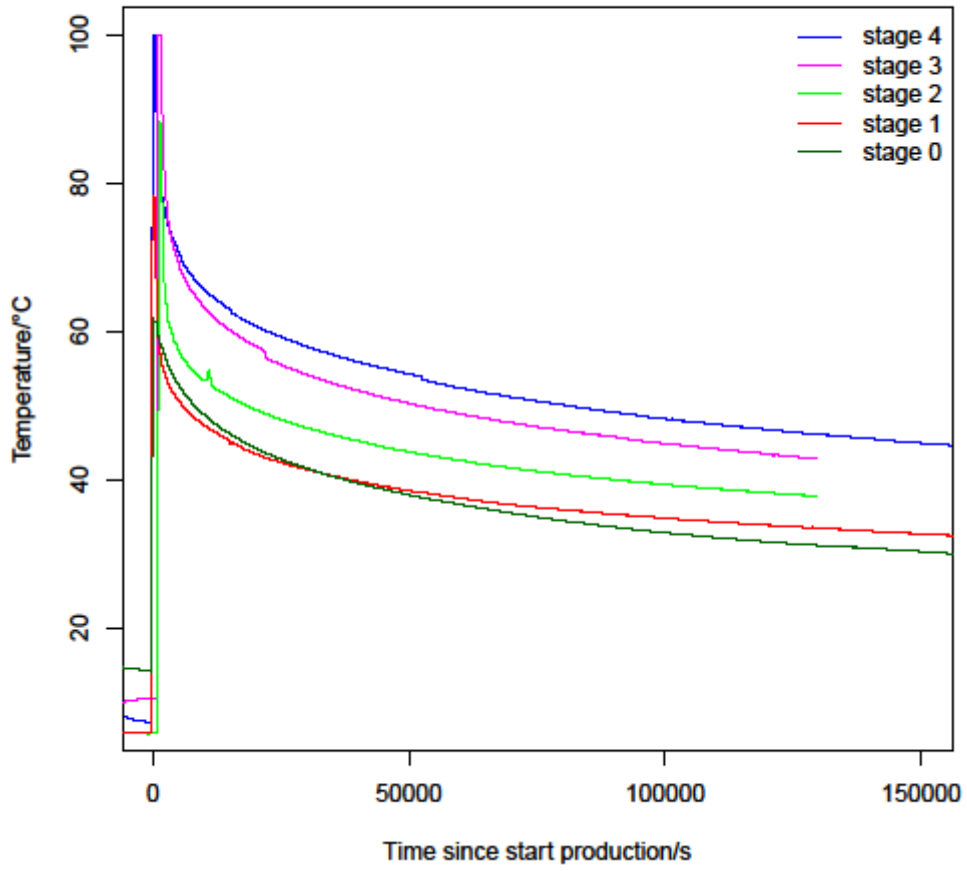

Figure 1: Temperature Development (stage 0-4)

The pressure at the top of the aquifer was constant at 2.53 MPa throughout the storage test. There are no indications of an increase of the pressure which might have been caused by a local boundary of the aquifer. The constant pressure in the free flowing aquifer is remarkable, because the decrease of the viscosity as the temperature of the water increases should have caused an increase of the flow rate or, if the flow rate is constant, an increase of the pressure at top Malm. The experimental data suggest the effects of the viscosity are negligible in this setting which leads to the assumption of rather large flow paths.

The development of the electrical conductivity is shown in Fig. 2. After starting production EC increased immediately from 0.6 mS/cm (EC of tap water) to around 1 mS/cm. For all stages, a similar development can be seen in principal but stages 0 and 2 show lower maximum values. Additionally stage 0 shows a slower rate compared to the other stages. An increase of electrical conductivity suggests at one hand an influx of reservoir water (1.1 mS/cm) and at the other hand a higher mineralization due to dissolution of carbonates in the aquifer. The latter is likely caused by the high CO_2 content of the injected water. The assumption is, that the produced waters from stages 3 and 4 show the highest dissolution rates due to the highest injection temperatures and therefore the highest CO_2 content while the produced water from stage 1 contains a higher influx of reservoir water or an undersaturation of the injected tap water compared to stages 0 and 2. That assumption is supported by both, sodium as well as calcium ion concentrations.

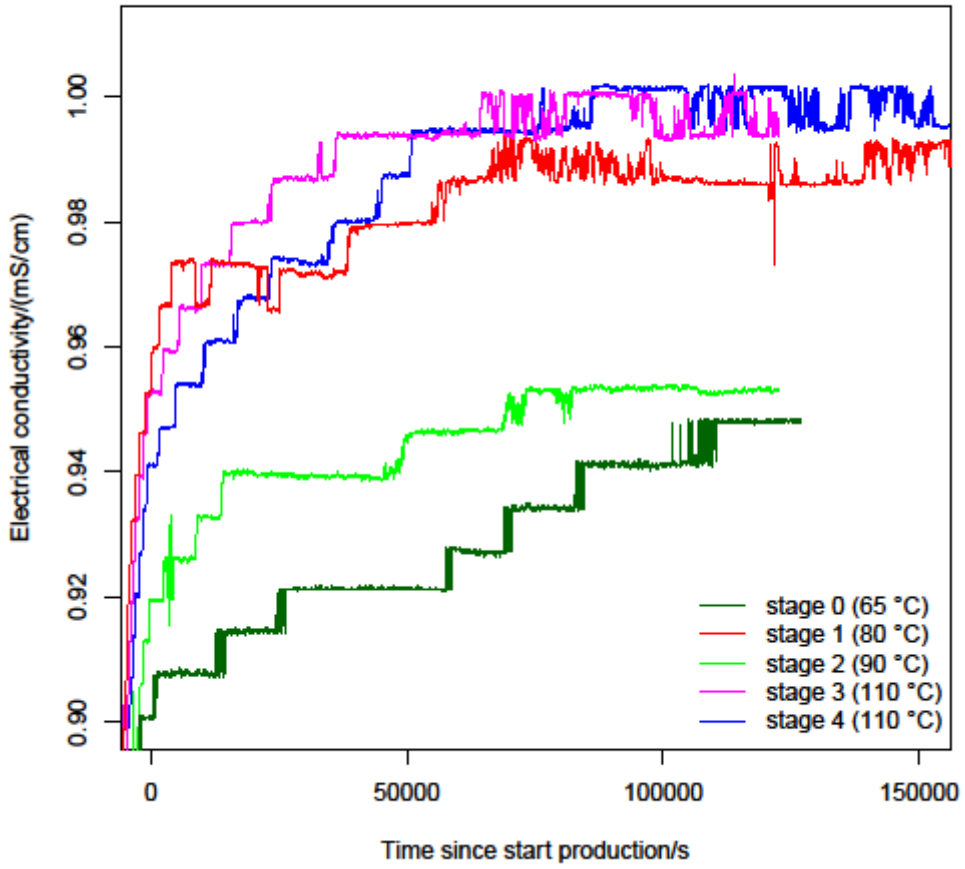

Figure 2: Development of EC (all stages)

3.2.2 Development of Hydrochemical Composition

The development of the sodium ion concentration for stages 1-4 is shown in Fig. 3. In general the sodium ion concentration is increasing sharply after the production started for each stage. There seems to be a correlation to the amount of injected water leaded to lower maximum concentrations for the later stages. The sodium ion concentration in the reservoir water is about 156 mg/L, whereas the concentration in tap water is 4 mg/L. Thus, the development of sodium ions serves like an additional chemical tracer that represents the influx of the reservoir water. The development of the sodium ion concentration for each stage can be described as a single exponential growth. The fit parameters represent the initial conditions and the dilution or influx rate. A similar behavior can be seen in the development of potassium ion concentration.

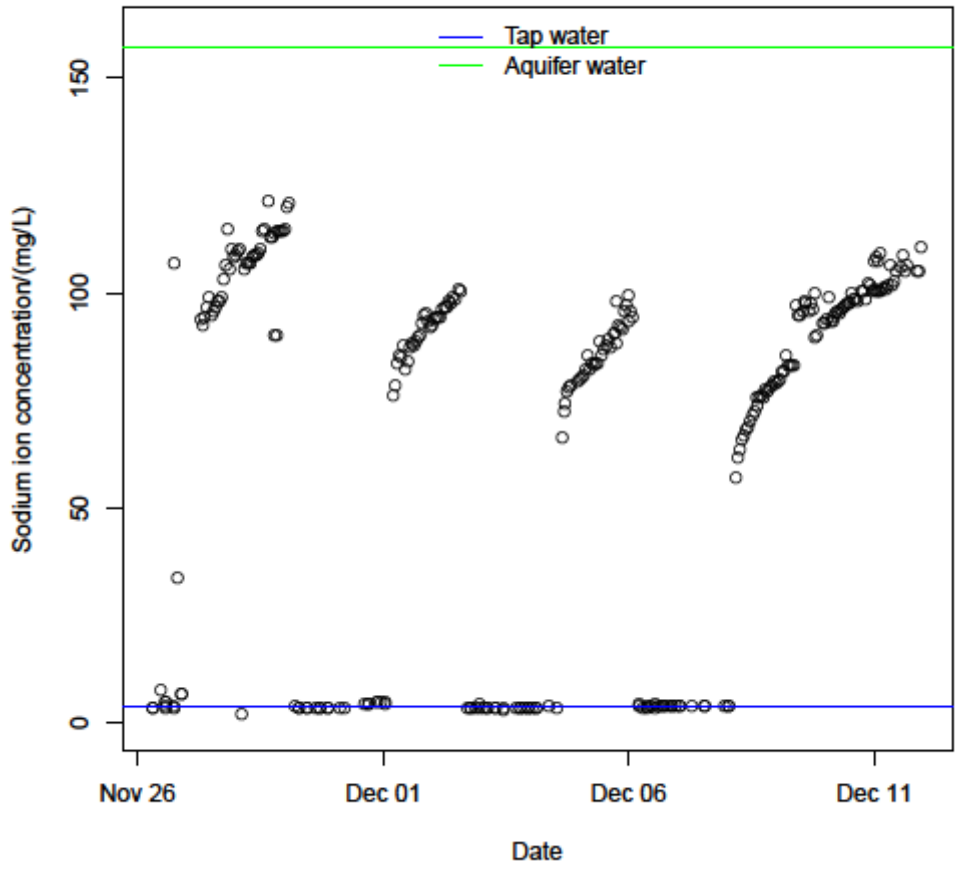

Figure 3: Development of the Sodium Ion Concentration (stage 1-4)

Figure 4 shows the development of the calcium ion concentration for stages 1-4. The calcium ion concentration for stage 1 and 2 decreases similarly over production time, and is converging to the lower cation concentration of the reservoir water. That indicates that neither significant dissolution nor precipitation processes occurred for these stages, which supports an accurate conditioning of the tap water with CO_2. During the third and fourth production stage as well as during the pre-test, calcium ion concentration also increase with time but exceed calcium ion concentration of the injected tap water and therefore suggests dissolution of carbonates in the aquifer. While calcium ion concentration of stage 0 and 4 converge towards the reservoir water concentration, the production time of stage 3 was too short. The development of the magnesium ion concentration is also converging to the magnesium ion concentration of the reservoir water. There are no evidences of significant dissolution processes of dolomite. Since the reservoir rock is mainly given by dolomite, these observations might not only be explained by the slower kinetics of dolomite but also with a primary injection into the upper limestone layer of the aquifer.

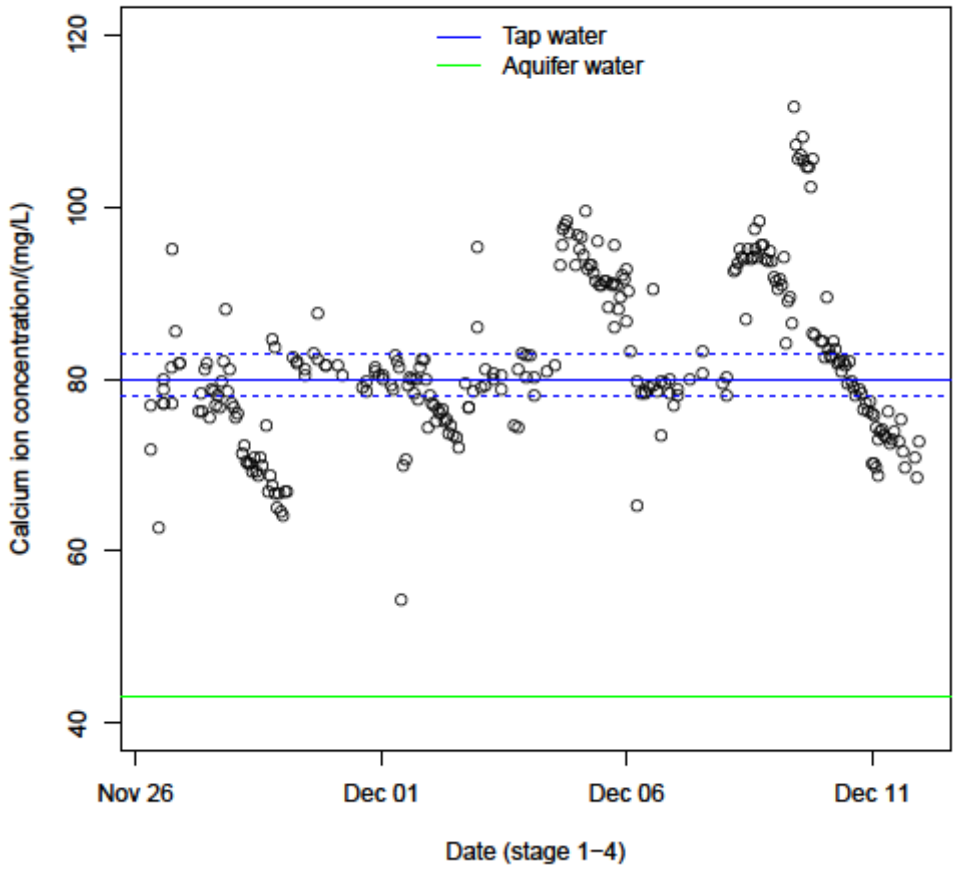

Figure 4: Development of the Calcium Ion Concentration (stage 1-4)

3.2.3 Tracer Breakthrough Curves

Figure 5 shows the tracer breakthrough curve (BTC) of sodium naphtionate during stage 3, exemplarily for all tracers. All maximum tracer concentrations were reached in less than three hours after the start of production and were followed by a strong tailing. Each injection of fluorescent dyes was followed by at least 7 hours of a chaser. Thus, the immediate production of fluorescent dyes was not to be expected (see e.g. Nordqvist et al. (2012)). The arrival time of the tracer assuming radial symmetric flow is highlighted in Fig. 5 in cyan.

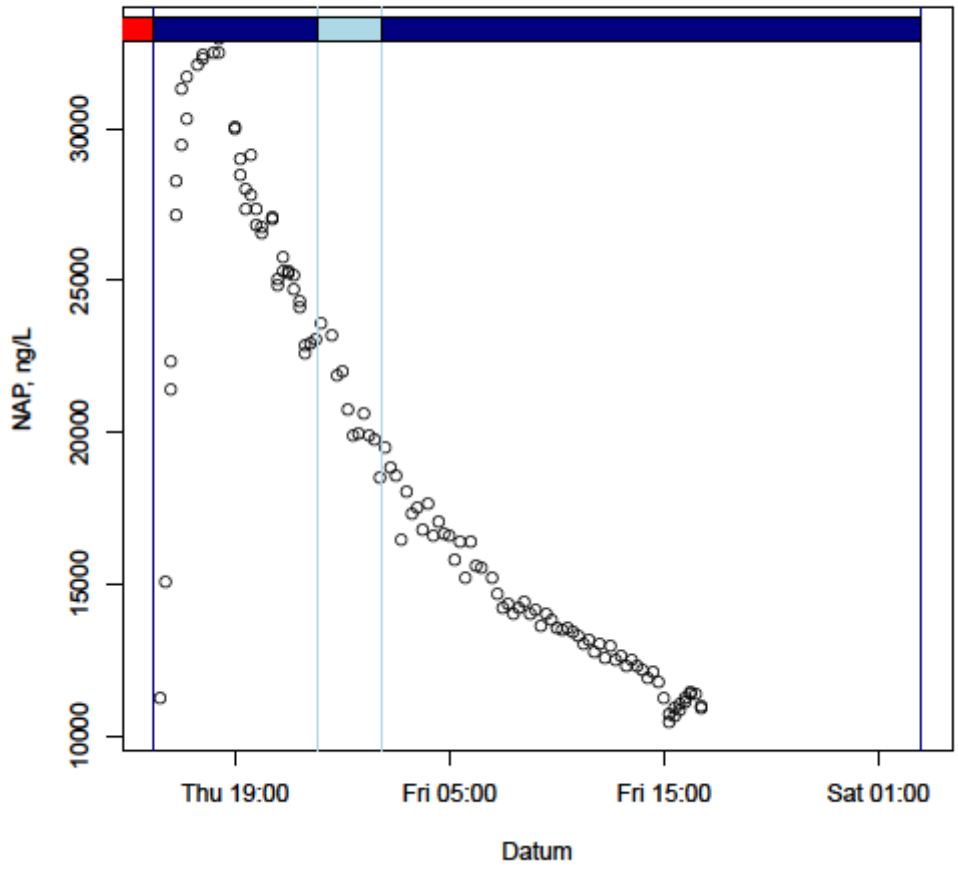

Figure 5: Breakthrough Curve of Na-Naphtionate (stage 3)

The recovery of the fluorescent dyes is given with 23 % up to 79 %, depending on the type of tracer. Different sorption behavior is the main reason for the strong variance of the recovery rates, but due to the high injection temperatures as well as high flow rates, the interaction of fluorescent dye and reservoir matrix is strongly reduced. Therefore it is hardly possible to suggest the specific surface that was available during the heat storage test. Breakthrough curves stated that the recovery is not finished after each stage. The development of the tracer concentrations is not explainable with the typically occurring radial symmetrical transport behavior of groundwater fluxes and it is not possible to interpret it by usual push-pull-tests. It is also not possible to explain the transport phenomena only by mixing processes during production. Therefore the idea of laminar fluid flow has to be discarded and a turbulent flow regime with big flow paths in the aquifer seems more realistic. That leads to the idea of mixing of injected tap water and reservoir water in a big carstified structure. Such a geological structure is dominating the transport behavior and could also be the explanation for the drilling problems for a vertical length of 100 m. The assumed carstic structure is the only explanation for the immediate occurrence of the tracer maximum and the simultaneously high concentration of sodium ions (see Fig. 3 and 5).

3.3. Energy Balance

Energy balance of stages 1-4 of the heat storage test is shown in Fig. 6, based on the temperature development of the produced water. Red lines stand for injected temperatures and blue lines for the temperature abatement during production. With increasing production stages the recovery of heat energy is also increasing. At the end of stage 4, it was possible to recover 48 % of the injected heat energy - despite the influx of cold reservoir water - while heat recovery of stage 0 was 35 %.

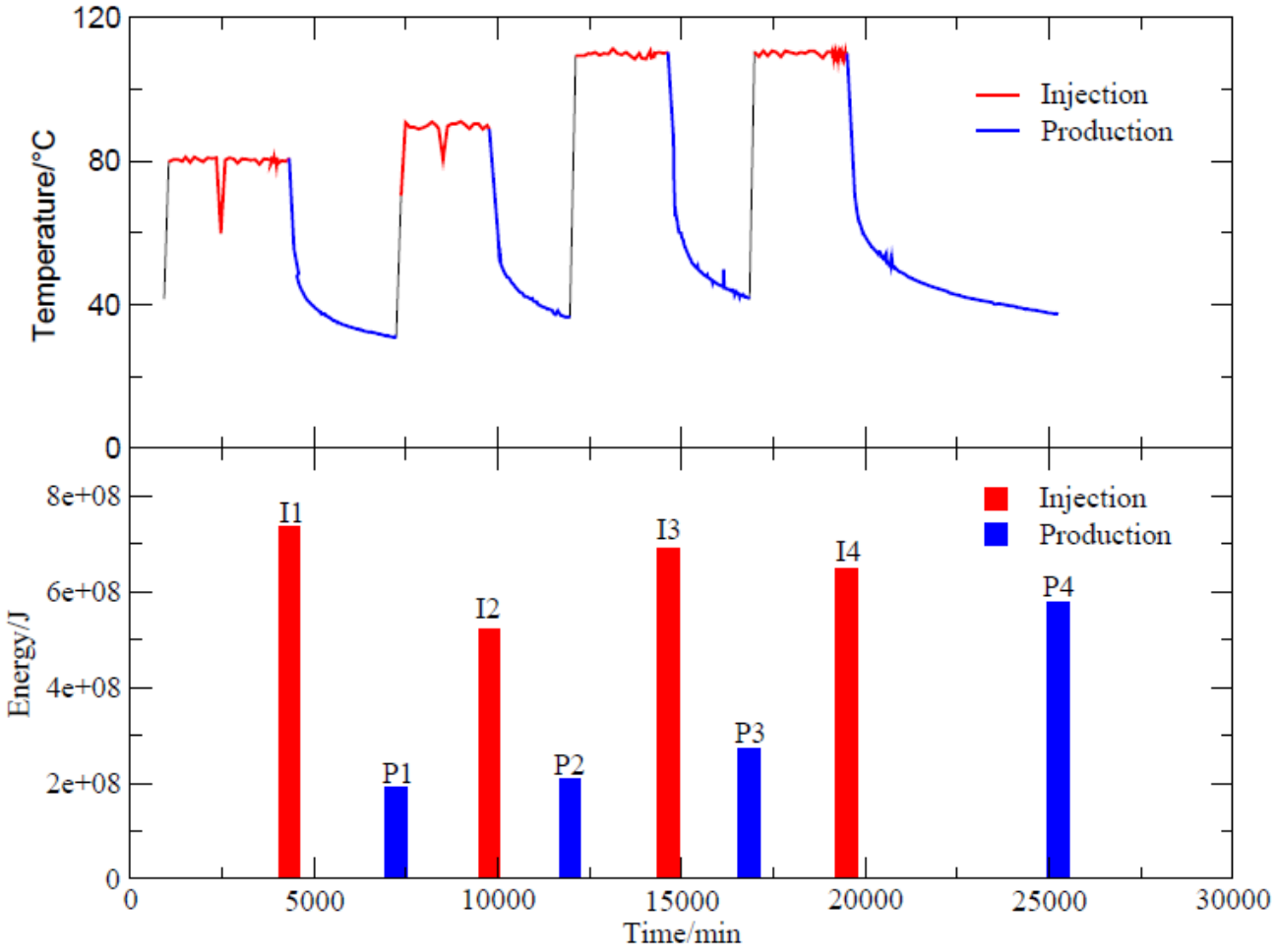

Figure 6: Energy Balance Based on Temperature Development (stages 1-4)

3.4 Temperature Correction

The very high permeabilities that were found in the aquifer were not expected by exploration methods and caused a free discharge of up to 19.4 L/s. Since the injected flow rate was set to 15 L/s, an immediate mixture of the injected hot water and the cold reservoir water took place instead of the assumed radial symmetrical flow of the injected hot tap water. That caused not only drilling problems, but also lower production temperatures. Therefore, a temperature correction was applied that describes the development of the produced temperatures without the influx of the cold reservoir water. As seen in Fig. 3, the development of the sodium ion concentration indicates an influx of reservoir water. This development was fitted for each stage and the resulting equation was used to correct the influence of the inflowing cold reservoir water on the temperature evolution. The temperature correction is shown exemplarily for stage 0. Figure 7 shows the temperature development of stage 0, indicating injection time (red bar) and production time (blue bar). Two sharp abatements are seen during injection and one during production stage which shows the moment of calibrating the measuring probes. Immediately after start production strong temperature abatement can be seen within the first minutes. At the end of production stage 0 (T_{Inj} = 65 °C), the uncorrected temperature is 31.3 °C. The development of the sodium ion concentration is fitted by assuming a single exponential growth converging to the concentration in the reservoir and shown in figure 8. This behavior reflects the dilution of the aquifer and thus, by means of that equation the influx of the cold reservoir water (21.7 °C) can be subtracted. The corrected temperature development is shown in Fig. 9, resulting in a corrected temperature which is about 15 K higher than the uncorrected temperatures. Temperature correction is essential for further calculations since the flow rate of normal operation is planned with 80 L/s and the injection period is over several months, which means the influx of the cold reservoir water will likely be negligible. It should be highlighted that the temperature of stage 4 is higher than in stage 3 after the same production time, although the injection temperatures were identical for both stages. That effect is also seen in the non-corrected temperature developments and is caused by the heating of the aquifer.

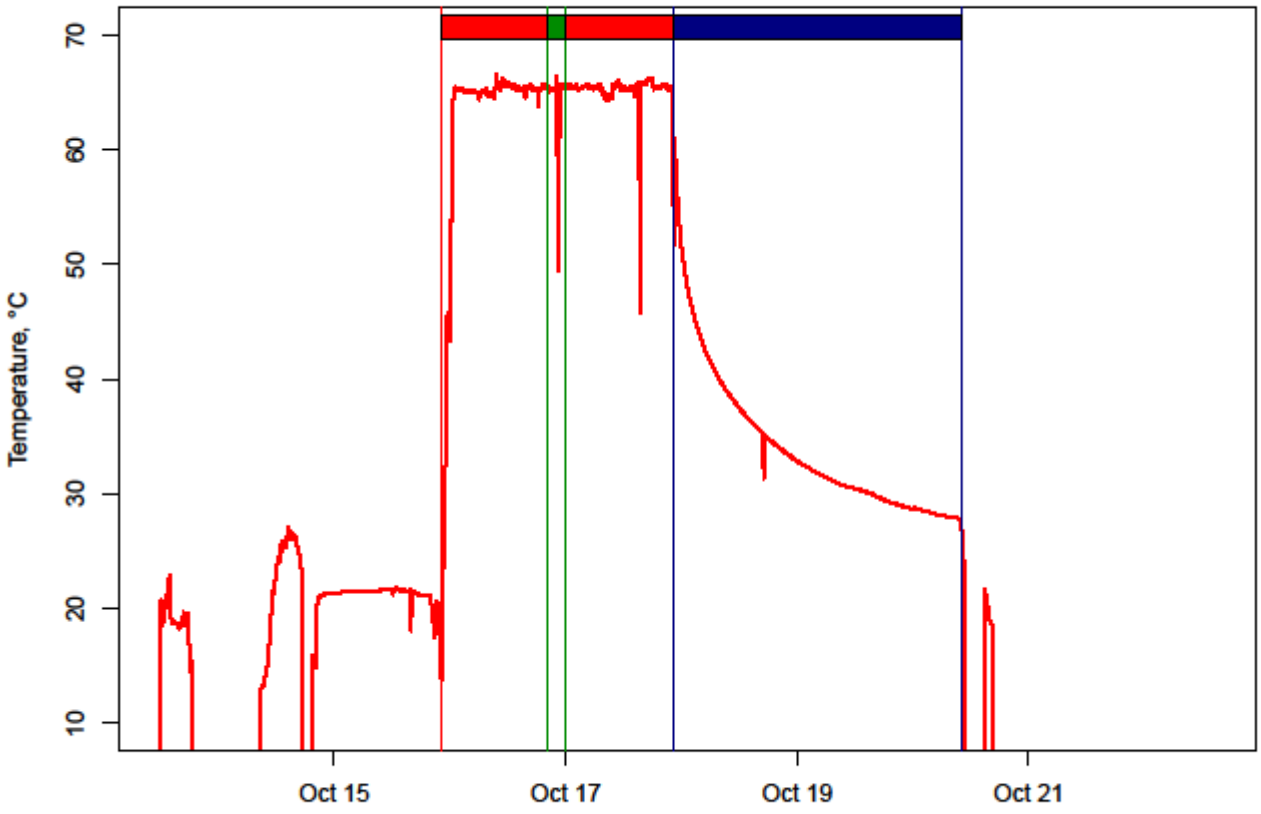

Figure 7: Temperature Development (stage 0)

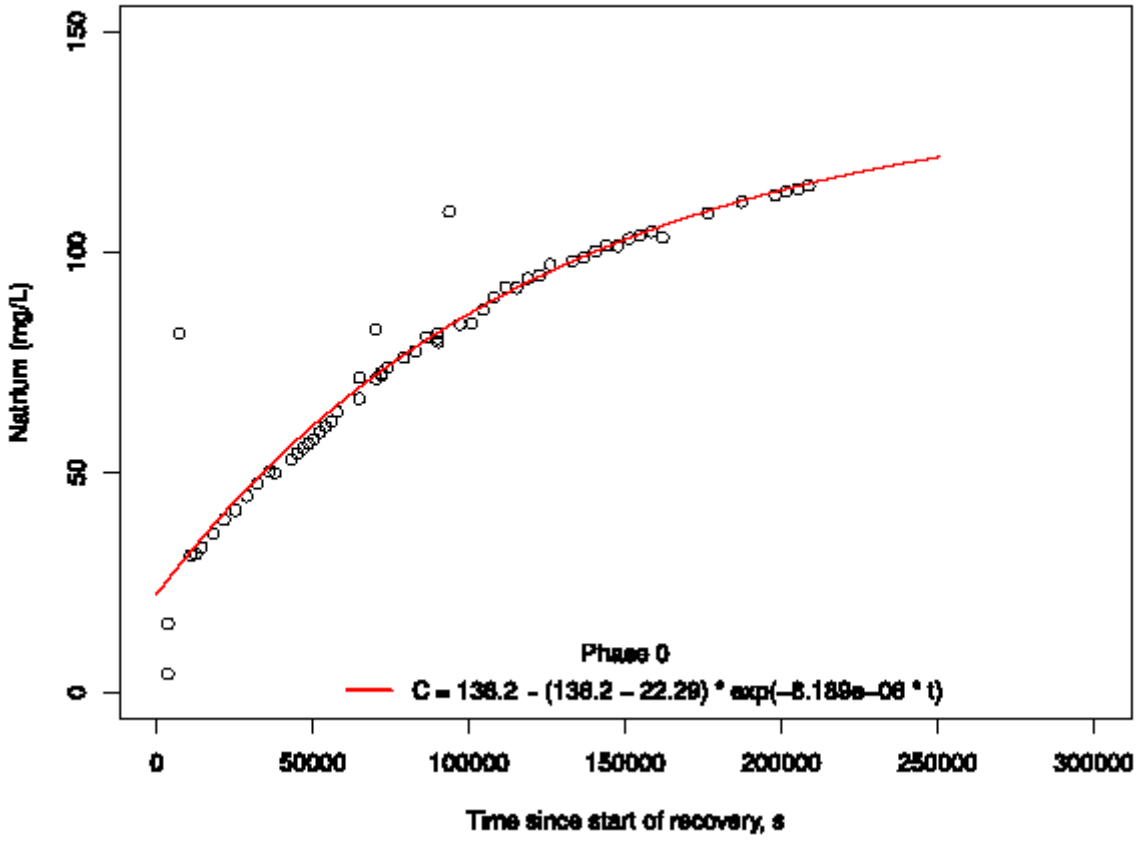

Figure 8: Fit of the Sodium Ion Concentration

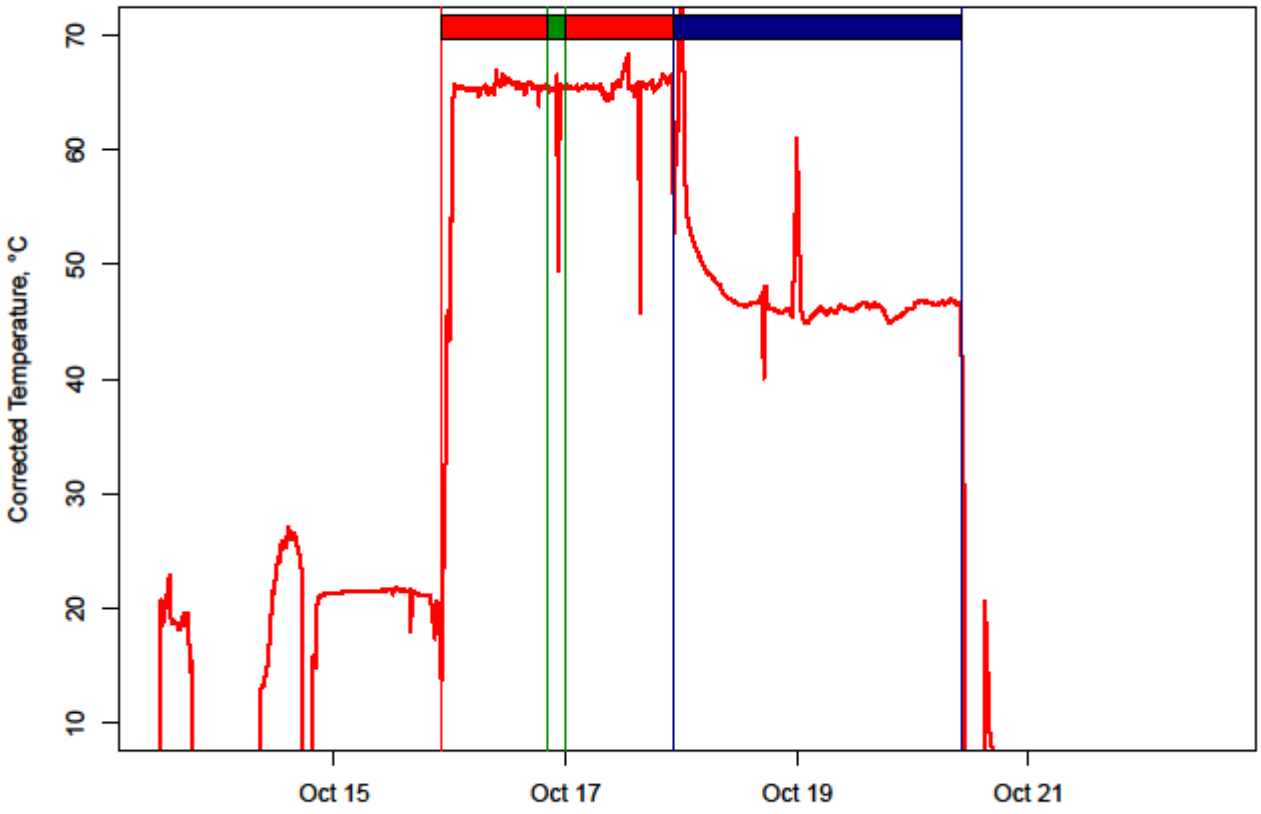

Figure 9: Corrected Temperature Development (stage 0)

4. CONCLUSION

Although the hydraulic tests showed an unusual high transmissivity and the investigation of the core samples indicated a high porosity, neither the evaluation of the hydraulic tests nor the hydrogeological model were able to predict the mixing of the injected water in the reservoir correctly. While the results of the hydrochemical monitoring suggests either mixing of tap and reservoir water during production or a contribution of reservoir water from a deeper strata not affected by injection stages, the tracer results removed this ambiguity and clearly indicate that mixing in the vicinity of the borehole occurs. Taking the slower reaction kinetics for dolomite into account, the Ca/Mg ratio is not sufficiently sensitive to distinguish whether the main part of the hot water was injected into the limestone alone or into both, limestone and dolomite. However, the hydrochemical characteristics of the reservoir water indicate that the limestone has a spatially limited extent and is not relevant for large scale groundwater flow. All together the results support the setup of a large scale ATES system at this site. The evaluated data of the large scale heat storage test calibrates the conceptual model with *PhreeqC* and enables future scenarios. Due to drilling problems logging data were not available to investigate groundwater flow geophysically. Data based on the hydraulic situation strongly orientates on the hydrochemical investigations and therefore numerical models of the test side have to make use of the hydrochemical investigations. To enable a prediction about the heating of the aquifer a temperature correction considering the influx of the cold reservoir water was mandatory and in this case only possible with hydrochemical data. Further research is needed to validate the hypothesis of peripheral precipitation during production when colder water (now in equilibrium with the reservoir) is heated in the aquifer.

REFERENCES

Böhm, F., and Koch, R., and Höferle, R., and Baasch, R.: Der Malm in der Geothermiebohrung Pullach Th2 – Faziesanalyse aus Spülproben (München, S-Deutschland), *Geologisches Blatt NO-Bayern*, **Heft 1-4**, (2010).

Drijver, B., and van Aarssen, M., and de Zwart, B.: High-Temperature Aquifer Thermal Energy Storage (HT-ATES): Sustainable and Multiusable, *Proceedings,* International Conference on Energy Storage, (2012).

Griffioen, J. and Appelo, C.A.J.: Nature and Extent of Carbonate Precipitation during Aquifer Thermal Energy Storage, Applied *Geochemistry*, **8**, (1993), 161-176.

Kasnavia, T., and Vu, D. and Sabatini, D.A.: Fluorescent Dye and Media Properties Affecting Sorption and Tracer Selection, *Groundwater*, **37**, (1999).

Hebig, K.H., and Zeilfelder, S., and Ito, N., and Machida, I., and Marui, A., and Scheytt, T.J.: Study of the Effects of the Chaser in Push-pull Tracer Tests by Using Temporal Moment Analysis, *Geothermics*, **54**, (2014), 43-53.

Hebig, K.H. and Ito, N., and Scheytt, T., and Marui, A.: Review: Deep Groundwater Research with Focus on Germany, *Hydrogeology Journal*, **20**, (2012), 237-251.

Nordqvist, R., and Hjerne, C., and Andersson, P.: Single-well and Large-scale Cross-hole Tracer Experiments in Fractured Rocks at Two Sites in Sweden, *Hydrogeology Journal*, **20**, (2012), 519-530.

Yang, S.Y. and Yeh, H.D. and Li, K.Y.: Modelling Transient Temperature Distribution for Injecting Hot Water Through a well into an Aquifer Thermal Storage System, *Geophysics Journal International*, **183**, (2010), 237-251.

Schmidt, D.U., and Leinfelder, R.R., and Schweigert, G.: Stratigraphy and Paleoenvironments of the Upper Jurassic of Southern Germany – A Review, *Zitteliana,* (2005), 31-41.